Revisiting Theoretical Limits for One Degree-of-Freedom Wave Energy Converters

Nathan M. Tom
National Renewable Energy Laboratory,
15013 Denver West Parkway,
Golden, CO 80401
e-mail: Nathan.Tom@nrel.gov

This work revisits the theoretical limits of one degree-of-freedom wave energy converters (WECs). This work considers the floating sphere used in the OES Task 10 WEC modeling and verification effort for analysis. Analytical equations are derived to determine bounds on displacement amplitude, time-averaged power (TAP), and power-take-off (PTO) force. A unique result found shows that the TAP absorbed by a WEC can be defined solely by the inertial properties and radiation hydrodynamic coefficients. In addition, a unique expression for the PTO force was derived that provides lower and upper bounds when resistive control is used to maximize power generation. For complex conjugate control, this same expression only provides a lower bound, as there is theoretically no upper bound. These bounds assist in comparing the performance of the floating sphere if it were to extract energy using surge or heave motion. The analysis shows because of differences in hydrodynamic coefficients for each oscillating mode, there are different frequency ranges that provide better power capture efficiency. The influence of a motion constraint on TAP while utilizing a nonideal power take-off is examined and found to reduce the losses associated with bidirectional energy flow. The expression to calculate TAP with a nonideal PTO is modified by the electrical conversion efficiency and the ratio of the PTO spring and damping coefficients. The PTO spring and damping coefficients were separated in the expression, allowing for limits to be set on the PTO coefficients to ensure net power generation. [DOI: 10.1115/1.4049287]

Keywords: alternative energy sources, energy conversion/systems, energy systems analysis, renewable energy, wave energy converters

1 Introduction

Over the last 45 years since the publication of Salter's foundational paper on wave power [1], research and development in wave energy technologies have pushed forward in hopes of bringing the industry closer to commercialization. In the last two decades, the worldwide marine and hydrokinetic industry has seen growth in investment and research awards; however, it can be argued that the industry as a whole remains in the early stages of technology development. To date, there are still no commercially grid-connected wave energy converters (WECs) installed in the United States, with only a few megawatts installed worldwide [2]. A significant challenge with WEC technology is the conversion of slow, irregular, and high-force oscillatory motion that must be converted to an output power signal with acceptable quality for a utility grid network [3].

The marine energy industry continues to explore a great number of designs ranging in scale from novel concept to oceangoing constructions. Therefore, development funds can be spread thin across a diverse research portfolio indicating a structured innovation approach maybe required to facilitate a convergence in WEC design and operation [4]. Although there are many different forms, WECs can generally be divided into three predominant classifications: (1) attenuator, most notably the Pelamis [5] and most recently Mocean's Blue Horizon [6], (2) point absorber, most notably Wavebob [7], Ocean Power Technologies PowerBuoy [8], while more recently Corpower Ocean [9], and (3) terminator, most notably the Wave Dragon [10]. Within these classifications, WEC devices can be further defined based on the mode of motion used to capture energy, such as point absorbers, oscillating wave surge converters [11], oscillating water columns [12], overtopping devices, and bulge wave devices [3].

Of all of the WEC concepts, the most common and well-studied design is the point absorber, which typically has a narrow-banded response; therefore, control is generally required to improve energy capture [13]. Often point absorbers are designed such that their resonance frequency aligns with the dominant wave frequency of the most frequently occurring sea states. This condition amplifies the WEC response to maximize power capture; however, the device response can drop dramatically when moving to higher or lower wave frequencies. As such, one of the unique aspects of optimal control for WECs [14] is the use of the power-take-off (PTO) to induce an artificial resonance by incorporating a spring term in the controller feedback law resulting in the reversal of energy flow requiring a PTO unit that can act as both a generator and a motor. Several studies have explored the optimal control of WECs when prohibiting the PTO from injecting energy back into the WEC oscillation. These strategies are commonly known as declutching [15] when the WEC oscillates at a higher frequency than its resonance frequency and clutching [16] when the WEC oscillates at a lower frequency than its resonance frequency. These control strategies are highly nonlinear that either disconnect the PTO to speed up the WEC or lock motion through the PTO to slow down the WEC to move the WEC velocity in phase with the wave excitation force. The topic of WEC control remains an area of significant interest in the marine energy industry with recent popular adoption of state-constrained optimization techniques that can handle nonlinear constraints often found in WEC designs [17–19].

Often the point absorber is assumed to oscillate in heave with the wave elevation profile given the common buoy-like and bottom-referenced device concepts [20]. However, as discussed in Ref. [21], the hydrodynamic radiation and diffraction forces

Contributed by the Advanced Energy Systems Division of ASME for publication in the JOURNAL OF ENERGY RESOURCES TECHNOLOGY. Manuscript received August 27, 2020; final manuscript received November 20, 2020; published online January 22, 2021. Assoc. Editor: Ben Xu.

between surging, similar for pitch, and heaving devices have different frequency responses that influence the effective energy capture bandwidth. For example, it has been shown that the theoretical upper limit on power captured by a surging or pitching device is twice that of a heaving device because of the asymmetric wave radiation pattern [22].

This paper builds off the work of Ref. [21] by extending the performance metric comparison to the required displacement amplitude and PTO force, and considering nonideal conversion efficiency. After introducing the floating WEC used in this analysis, the author provides a discussion of the differences in the hydrodynamic and radiation coefficients. This is followed by deriving the upper bound on the amplitude of displacement for each mode of motion, highlighting how constraints such as the PTO stroke length can reduce the energy capture potential. Next, we discuss the influence of the hydrodynamic radiation coefficients on maximum power capture using complex conjugate [13] or resistive PTO control. This is followed by deriving the upper and lower bounds of the PTO force requirement, which depends on the control strategy implemented. Finally, we provide a discussion on how improvements in maximum power capture can be degraded by nonunity PTO efficiency, which can be aggravated based on the mode of oscillation.

2 Floating Body Description

For this study, we selected the floating sphere used for the Ocean Energy Systems Task 10 Wave Energy Converter modeling and verification effort [23]. The floating sphere has a radius of 5.0 m, and its origin is located on the mean water surface at the center of the spherical body, with a summary of the model parameters provided in Table 1. The mass of a floating half-submerged sphere is given by

$$m = \frac{2\rho\pi r^3}{3} \tag{1}$$

where ρ is the fluid density and r is the sphere radius. The linearized heave hydrostatic spring coefficient is modeled by the following expression:

$$C_{33} = \rho g A_{wp} = \rho g \pi r^2 \tag{2}$$

where A_{wp} is the water plane area. A free floating body will not have a hydrostatic restoring coefficient in surge; however, for station keeping an external spring, such as mooring or PTO control strategies, it will need to be coupled to the surge degree of motion. For this analysis, we assumed that the floating sphere could be connected to a fixed reference frame by an external spring with a magnitude equal to the heave hydrostatic restoring coefficient (i.e., $C_{11} = C_{33}$).

The hydrodynamic coefficients used in the analysis to estimate the displacement and power absorption of the sphere were obtained from WAMIT [24] and are plotted in Fig. 1. As shown in Fig. 1(*a*), for heave oscillation the radiation wave damping peaks at a lower wave frequency than surge and the same for the added mass; however, for surge, the wave damping peak corresponds with a greater drop from the added mass peak than heave, which will be highlighted in a later section. For the wave-excitation force

Table 1 General properties of the floating sphere [23]

Parameters	Variable	Assigned values
Radius of sphere	r	5 m
Center of gravity	c_g	0.0, 0.0, −2.0 m
Center of buoyancy	c_b	0.0, 0.0, −1.875 m
Mass of sphere	m	261.8×10^3 kg
Water depth	m	Infinite m
Water density	ρ	1000 kg/m^3

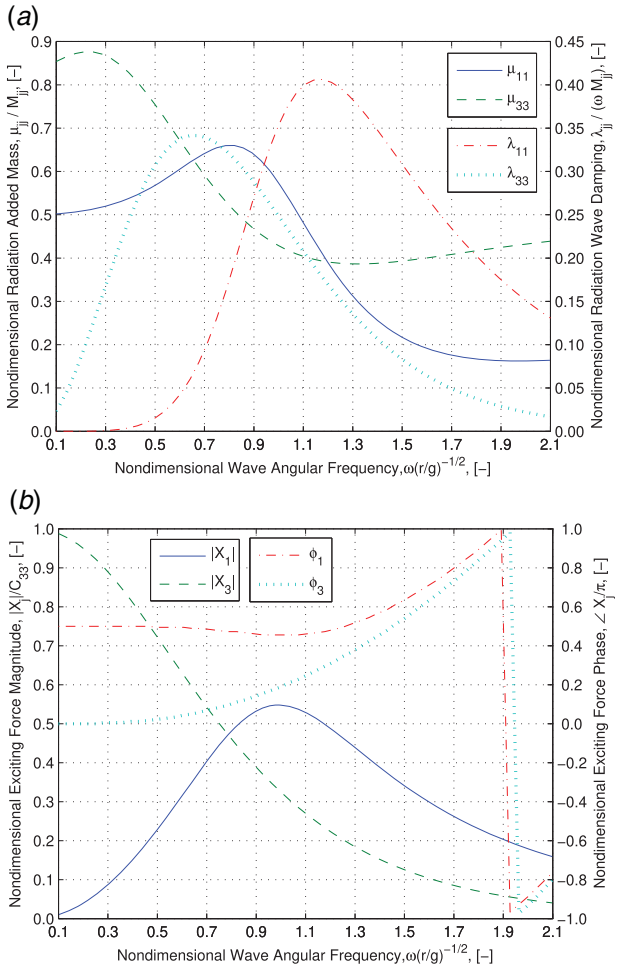

Fig. 1 Nondimensional hydrodynamic surge and heave radiation and wave-excitation force coefficients for the floating sphere: (*a*) radiation added mass μ_{jj} and wave damping λ_{jj} and (*b*) wave-exciting force magnitude $|X_j|$ and phase ϕ_j

shown in Fig. 1(*a*), in heave the force is maximum at the lowest frequencies and continues to decrease as the wave frequency increases. While in surge, the wave-excitation force tends to zero at the upper and lower frequencies while peaking in the intermediate frequency regime. As will be discussed in Sec. 4.2, as the WEC motion becomes more heavily constrained, the peak in power capture centers on the peak in the wave-excitation force rather than at the resonant frequency.

3 Regular Wave Analysis

In floating body dynamics, it is common practice to understand the frequency response of the device by analyzing the response under sinusoidal waves, in which the wave elevation profile is modeled by

$$\eta(x, t) = A\cos(\omega t - kx) = \Re\left\{Ae^{i\omega t}\right\} \tag{3}$$

where A is the wave amplitude, k is the wave number, η is the wave elevation, and ω is the wave angular frequency. The mechanical force from the PTO system will be modeled by

$$f_{PTOj} = -\Re\left[\left(\lambda_g - iC_g/\omega\right)i\omega\xi_j e^{i\omega t}\right] \tag{4}$$

where C_g is the PTO-restoring coefficient, λ_g is the PTO-damping coefficient, and ξ_j is the j degree-of-freedom complex amplitude of motion where $j = 1$ and $j = 3$ corresponds to surge and heave motion, respectively,

The frequency-domain expressions for the hydrostatic, radiation, diffraction, and PTO forces can be inserted into the one degree-of-freedom equation of motion to derive the displacement and velocity response amplitude operators of the floating sphere:

$$\frac{\xi_j}{A} = \frac{X_j}{\left[C_{jj} + C_g - \omega^2\left(M_{jj} + \mu_{jj}\right)\right] + i\omega\left[\lambda_{jj} + \lambda_g\right]} \tag{5}$$

$$\frac{i\omega\xi_j}{A} = \frac{X_j}{\left[\lambda_{jj} + \lambda_g\right] + i\left[-\left(C_{jj} + C_g\right)/\omega + \omega\left(M_{jj} + \mu_{jj}\right)\right]} \tag{6}$$

where X_j is the wave-exciting force per wave amplitude, C_{jj} is the linear spring coefficient in the jth degree-of-freedom, M_{jj} is the mass or moment of inertia in the jth degree-of-freedom, μ_{jj} is the radiation added moment of inertia or added mass or in the jth degree-of-freedom, and λ_{jj} is the radiation wave damping in the jth degree-of-freedom.

The magnitude of Eq. (5) will be taken to obtain motion amplitude bounds:

$$\begin{aligned}\left|\frac{\xi_j}{A}\right| &= \frac{|X_j|}{\sqrt{2}\omega\lambda_{jj}} \frac{1}{\Xi_j\sqrt{1+\frac{1}{\Xi_j}}} \\ &= \frac{4\varepsilon\rho g V_g}{\sqrt{2}\omega k|X_j|} \frac{1}{\Xi_j\sqrt{1+\frac{1}{\Xi_j}}}, \quad \varepsilon = \begin{cases} 1 & \text{for } j=3 \\ 2 & \text{for } j=1,5 \end{cases}\end{aligned} \tag{7}$$

where V_g is the wave group velocity, and the Haskind expression [25] has been substituted in the second line of Eq. (7). Ξ is a measure of the ratio between the inertial and resistive forces that arise from WEC oscillation and is defined by

$$\Xi_j = \sqrt{1 + \left[\frac{C_{jj} + C_g - \omega^2\left(M_{jj} + \mu_{jj}\right)}{\omega\lambda_{jj}}\right]^2} \tag{8}$$

Because the bracketed term in Eq. (8) is squared, Ξ will be bounded between 1 and ∞; see Fig. 2. The lower bound will be obtained when the spring forces cancel the acceleration forces, and if no phase control is implemented, $C_g = 0$ occurs only at the resonance

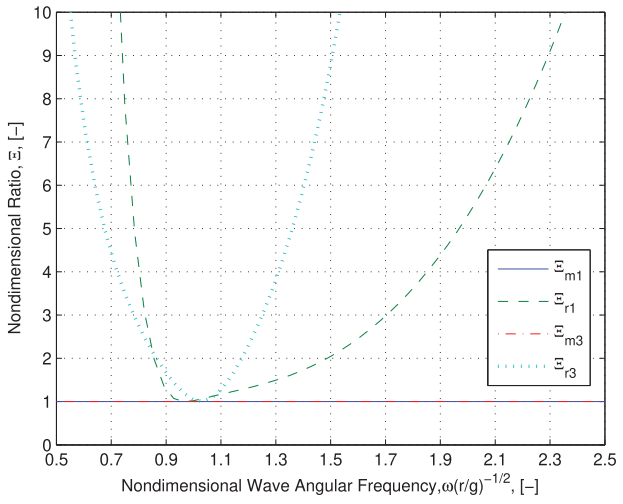

Fig. 2 The values of Ξ, given by Eq. (8), which is a measure of the ratio between inertial/spring and resistive forces that are generated because of WEC oscillations. The subscript *m* refers to maximum power absorption, and the subscript *r* refers to the maximum power absorption under resistive control when setting $C_g = 0$.

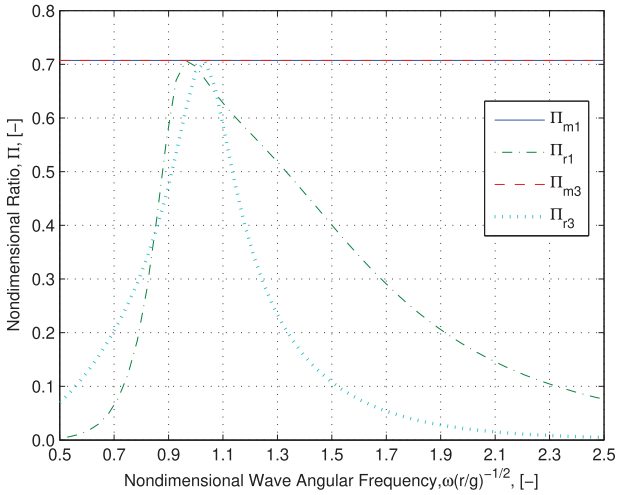

Fig. 3 The values of Π, defined in Eq. (9). The subscript *m* refers to maximum power absorption, and the subscript *r* refers to the maximum power absorption under resistive control when setting $C_g = 0$.

frequency of the WEC. Furthermore, it has also been assumed that the PTO linear damping coefficient has been selected, such that $\lambda_g = \lambda_{jj}\Xi$. The reason behind this selection will be described in the following section. If deep water is assumed, $kh \geq \pi$, then Eq. (7) can be simplified to the following form:

$$\begin{aligned}\left|\frac{\xi_j}{A}\right| &= \frac{2\varepsilon\rho g}{\sqrt{2}k^2|X_j|} \underbrace{\frac{1}{\Xi_j\sqrt{1+\frac{1}{\Xi_j}}}}_{\Pi} = \frac{2\varepsilon\rho g^3}{\sqrt{2}\omega^4|X_j|}\Pi \\ &= \frac{\varepsilon\rho g\lambda_w^2}{2\sqrt{2}\pi^2|X_j|}\Pi, \; \varepsilon = \begin{cases} 1 & \text{for } j=3 \\ 2 & \text{for } j=1,5 \end{cases}\end{aligned} \tag{9}$$

where λ_w is the wavelength and h is the water depth. Because Eq. (8) is bounded between $[1, \infty]$, the term, Π, in Eq. (9) is bounded between $\left[0, 1/\sqrt{2}\right]$, see Fig. 3. The upper bound on the motion response is set by the following expression:

$$\left|\frac{\xi_j}{A}\right|_{\max} = \frac{\varepsilon\rho g\lambda_w^2}{4\pi^2|X_j|}, \quad \varepsilon = \begin{cases} 1 & \text{for } j=3 \\ 2 & \text{for } j=1,5 \end{cases} \tag{10}$$

Therefore, the maximum displacement amplitude, in deep water, is relative to the wavelength squared and inversely proportional to the wave-exciting force/torque.

If shallow water is assumed, $kh \to 0$, then Eq. (7) can be simplified to the following form:

$$\left|\frac{\xi_j}{A}\right|_{\max} = \frac{2\varepsilon\rho g^2 h}{\omega^2|X_j|}, \quad \varepsilon = \begin{cases} 1 & \text{for } j=3 \\ 2 & \text{for } j=1,5 \end{cases} \tag{11}$$

The maximum motion displacement amplitude in shallow water is proportional to the water depth, and inversely proportional to the wave-exciting force and to the square of the wave angular frequency.

When comparing the velocity amplitudes between surge and heave in deep water for maximum power capture, see Fig. 4; for wave frequencies below the resonance frequency, surge outpaces heave. Above the resonance frequency, the surge oscillation requires a smaller amplitude compared to heave that is consistent with Eq. (10), as the wave-excitation force is one variable that differs between the two oscillation modes. Referring back to Fig. 1(*b*), one can see that the surge wave-excitation force is

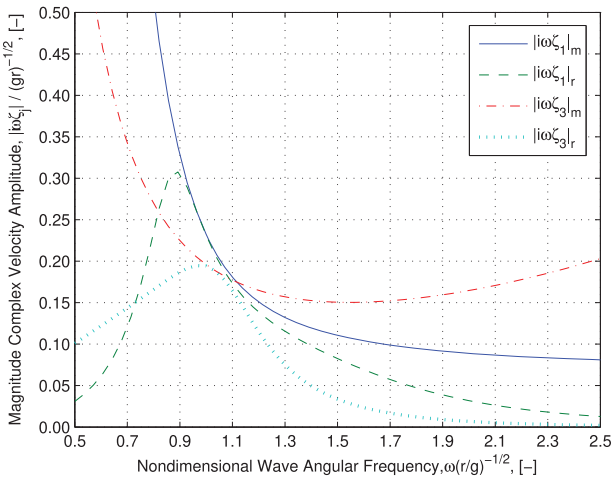

Fig. 4 Nondimensional surge and heave velocity response amplitude operators for the floating sphere. The subscript *m* refers to maximum power absorption, and the subscript *r* refers to the maximum power absorption under resistive control when setting $C_g = 0$.

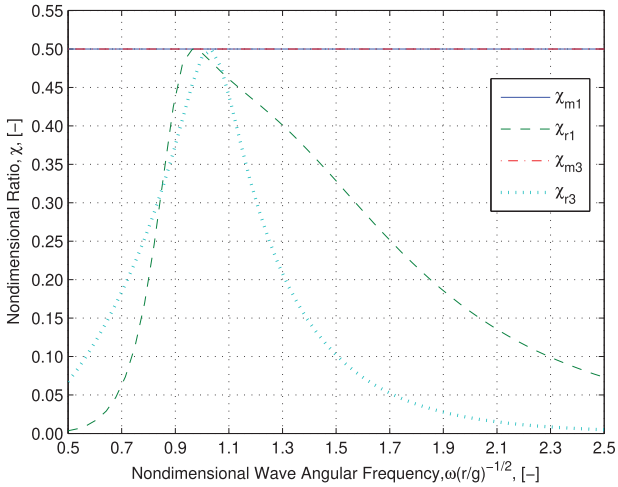

Fig. 5 The values of χ, defined in Eq. (15). The subscript *m* refers to maximum power absorption, the subscript *r* refers to the maximum power absorption under resistive control when setting $C_g = 0$.

larger than heave for higher frequencies and will reduce the required displacement amplitude.

4 Time-Averaged Power Absorption

The maximum time-averaged power absorbed by a WEC oscillating in a single degree-of-freedom [22] can be modeled by the following:

$$\frac{P_{Tj}}{A^2} = \frac{\lambda_g \left| i\omega\xi_j \right|^2}{2} = \frac{1}{4}\frac{|X_j|^2}{\lambda_{jj}} \frac{1}{1+\sqrt{1+\left(\dfrac{C_{jj}+C_g-\omega^2\left(M_{jj}+\mu_{jj}\right)}{\omega\lambda_{jj}}\right)^2}}$$

$$= \frac{1}{4}\frac{|X_j|^2}{\lambda_{jj}} \frac{1}{1+\Xi_j} \tag{12}$$

Therefore, it is beneficial to minimize the variable Ξ ratio, which can be described by the following inequality:

$$\left(C_{jj}+C_g\right)/\omega - \omega\left(M_{jj}+\mu_{jj}\right) << \lambda_{jj} \tag{13}$$

As described earlier in the floating body description section, given that the hydrostatic restoring coefficient is static, then the power capture potential of the WEC will be greater when the radiation added mass is minimized and the wave damping is maximized. Thus, it may be possible to adjust the shape of a WEC at each wave frequency to meet the inequality by controlling the radiation added mass and wave damping coefficients.

The previously mentioned expressions require unconstrained motion, and the PTO linear damping coefficient takes the following value:

$$\lambda_g = \lambda_{jj}\sqrt{1+\left[\frac{C_{jj}+C_g-\omega^2\left(M_{jj}+\mu_{jj}\right)}{\omega\lambda_{jj}}\right]^2} = \lambda_{jj}\Xi \tag{14}$$

Equation (12) can be simplified further by substituting the Haskind expression as follows:

$$\frac{P_{Tj}}{A^2} = \frac{\varepsilon\rho g V_g}{k}\underbrace{\frac{1}{1+\Xi_j}}_{\chi}, \quad \varepsilon = \begin{cases} 1 & \text{for } j=3 \\ 2 & \text{for } j=1,5 \end{cases} \tag{15}$$

As shown by Eq. (15), the WEC time-averaged power can be defined solely by the inertial properties and the radiation hydrodynamic coefficients. The expression for the time-averaged power now requires fewer hydrodynamic coefficients to evaluate the maximum power potential of a given WEC. The power absorption of a floating body can be estimated from the value of χ, which is plotted in Fig. 5. In addition, the theoretical maximum power absorption limit for an axisymmetric device, which is oscillating in pitch or surge, is twice that of the heaving case [14,22].

The maximum power absorption from Eq. (15) is obtained when $\Xi_j = 1$, which occurs when the inertial and spring forces cancel. This condition is naturally met when the wave frequency matches the resonance frequency of the floating body [22]. As the wave frequency moves above or below the resonance frequency, an external positive or negative PTO spring, equal to $C_g = -[C_{jj} - \omega^2(M_{jj}+\mu_{jj})]$, must be added to the WEC system to obtain maximum power absorption and is often referred to as complex conjugate control [14]. Incorporating this controllable spring remains a current research interest in the wave energy field, with several efforts implementing the spring either mechanically or through control strategies. Because of the increased complexity related to incorporating a controllable spring, many developers have relied on resistive control by adjusting the PTO-damping coefficient, λ_g, which is equal to Eq. (14), when setting $C_g = 0$.

The power absorption obtained from complex conjugate and resistive control is equal at the floating body resonance frequency; however, it is of interest to develop a ratio between these two control strategies at other wave frequencies. The ratio can be calculated by taking the ratio of Eq. (15) when setting $\Xi_j = 1$ and with Ξ_j when $C_g = 0$, which provides the following expression:

$$\frac{P_{Tmj}}{P_{Trj}} = \frac{1+\Xi_{rj}}{2} = \frac{1+\sqrt{1+\left[\dfrac{C_{jj}-\omega^2\left(M_{jj}+\mu_{jj}\right)}{\omega\lambda_{jj}}\right]^2}}{2} \tag{16}$$

where the subscript m refers to maximum power absorption, whereas the subscript r refers to the maximum power absorption under resistive control, and Ξ_{rj} refers to setting $C_g = 0$ in Eq. (8). Equation (16) has been plotted in Fig. 6 and is unique in that it remains dependent only on the spring, inertial, and radiation coefficients. Furthermore, as shown in Fig. 6, when above the resonance frequencies, the ratio between complex conjugate and resistive control strategies is much lower for surge than in heave, whereas below resonance surge will quickly outpace heave. This

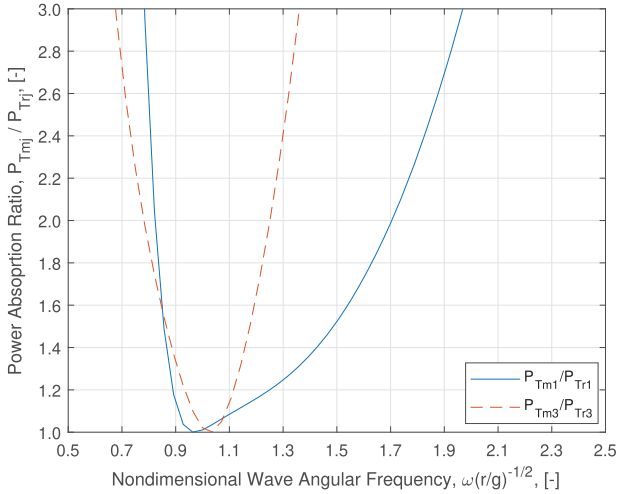

Fig. 6 Ratio of power absorption between complex conjugate and resistive control for the floating sphere.

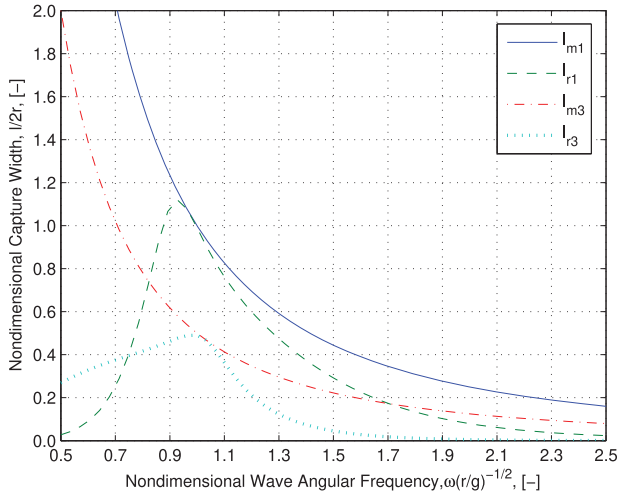

Fig. 7 The capture width of complex conjugate and resistive control nondimensionalized by the diameter of the floating sphere

performance can be attributed to the natural hydrodynamic bandwidth, which helps tune the power capture, as discussed in Ref. [21].

4.1 Incident Wave Power and Capture Width. The efficiency of a given WEC can be calculated once the wave power contained within a propagating wave is known. The wave-power-per-unit width, P_w, is estimated from the following expression:

$$\frac{P_w}{A^2}=\frac{1}{2}\rho g V_g=\frac{1}{4}\rho g\sqrt{\frac{g}{h}\tanh kh}\left[1+\frac{2kh}{\sinh 2kh}\right]\overset{kh\to\infty}{\approx}\frac{1}{4}\frac{\rho g^2}{\omega}=\frac{\rho g^2 T}{8\pi} \tag{17}$$

where T is the wave period. The capture width is normally defined as the ratio of the time-averaged WEC absorbed to the wave power and given as follows:

$$l_j=\frac{P_{Tj}}{P_w} \tag{18}$$

Equations (15) and (17) can be substituted into Eq. (18) to calculate the capture width of a given WEC:

$$l_j=\frac{\dfrac{\varepsilon\rho g V_g}{k}\dfrac{1}{1+\Xi_j}}{\dfrac{1}{2}\rho g V_g}=\frac{2\varepsilon}{k}\frac{1}{1+\Xi_j} \tag{19}$$

$$\max\ l_j=\frac{\varepsilon}{k}=\frac{\varepsilon\lambda_w}{2\pi},\quad \varepsilon=\begin{cases}1 & \text{for } j=3\\ 2 & \text{for } j=1,5\end{cases} \tag{20}$$

The maximum capture width is related to the wavelength, which theoretically implies that a WEC can absorb more incident wave power than contained within the WEC length that is perpendicular to the wave crest (see Fig. 7); however, it is well known that the required amplitudes of motion may not be physically achieved [22]. The results from Eq. (19) are limited to axisymmetric devices, but if the device characteristic length is small relative to the wavelength, the WEC could be assumed to be a point absorber with antisymmetrical wave radiation patterns [26].

4.2 Influence of Motion Constraints on Maximum Absorbed Power. The theoretical maximum WEC power absorption, given by Eq. (12), requires unconstrained motion and is known to require unrealistic amplitudes of motion. As observed from Eq. (10), the required displacement amplitude will quickly increase in longer wave periods [22], where the wavelength can be several hundred meters. Under sinusoidal motion, the maximum power absorption when considering a maximum motion amplitude, was explored in Ref. [27], which provides the following equation:

$$P_{Tj}=\begin{cases}\frac{1}{8}A^2|X_j|^2/\lambda_{jj} & \delta_j\geq 1\\ \frac{1}{2}A|X_j|\omega|\xi_j|_{\max}-\lambda_{jj}\omega^2|\xi_j|^2_{\max} & \delta_j<1\end{cases} \tag{21}$$

where $|\xi_j|_{\max}$ is the displacement amplitude limit, and δ is constrained-to-optimal velocity ratio given by

$$\delta_j=\frac{\omega|\xi_j|_{\max}}{A}\frac{2\lambda_{jj}}{|X_j|}=\frac{\omega|\xi_j|_{\max}}{A}\frac{k|X_j|}{2\varepsilon\rho g V_g} \tag{22}$$

To match the power output described earlier, for $\delta_j<1$, the required linear PTO coefficients are given by

$$\frac{\lambda_g}{\lambda_{jj}}=\begin{cases}1, & \delta_j\geq 1\\ \frac{A|X_j|}{\omega|\xi_j|_{\max}\lambda_{jj}}-1, & \delta<1\end{cases} \tag{23}$$

$$C_g=-\left[C_{jj}-\omega^2\left(M_{jj}+\mu_{jj}\right)\right] \tag{24}$$

If Eq. (21), with $\delta_j<1$, was substituted into the numerator of Eq. (18), the capture efficiency would be inversely proportional to the wave amplitude. For unrestricted motion, the capture efficiency will be the same regardless of wave amplitude, whereas for strongly restricted motion, the capture efficiency will decrease as the wave amplitude increases and become from a hydrodynamic perspective less efficient. In taking the limit, $\delta\to 0$, the absorbed power is optimized when the wave-exciting force/torque is greatest instead of at the resonance frequency [28].

4.3 Power-Take-Off Power Quality. The PTO instantaneous power [29] can be modeled by the following equation:

$$P_j(t)=\frac{\lambda_g|i\omega\xi_j|^2}{2}+\frac{|i\omega\xi_j|^2}{2}|Z|\cos\left(2\left(\omega t+\phi\right)+\nu\right) \tag{25}$$

where $Z=\lambda_g-iC_g/\omega$, ν is the phase of Z and ϕ is the phase of $i\omega\xi_j$. As observed in the second term in Eq. (25), if $C_g\neq 0$, the instantaneous power will oscillate between positive and negative, resulting in an energy flow reversal. The instantaneous PTO power peaks (P_{+j}) and the input reactive power (P_{-j}) are given by

$$P_{\pm j}=\frac{\lambda_g|i\omega\xi_j|^2}{2}\left[1\pm\sqrt{1+\left(\frac{C_g}{\omega\lambda_g}\right)^2}\right] \tag{26}$$

The peak-to-average power ratio can be obtained by dividing Eq. (26) by the time-averaged power, as shown in Eq. (12), leading to the following expression:

$$PA_{\pm j}=1\pm\sqrt{1+\left(\frac{C_g}{\omega\lambda_g}\right)^2} \tag{27}$$

Therefore, the PTO peak-to-average power ratio is defined only by the PTO coefficients and can be tuned to stay within the power capacity of the PTO. As observed from Eq. (27), there will be no bidirectional energy flow when $C_g=0$, preventing any negative instantaneous power. This condition is often referred to as resistive control, and the peak-to-average power ratio will be 2. The input power requirement, $C_g\neq 0$, is not required at the floating body resonance; however, moving away from resonance, the peak-to-average power ratio can increase dramatically, resulting in large energy flux reversals.

If bidirectional energy flow is allowed and the PTO force coefficients, C_g and λ_g, are selected such that the phase and amplitude conditions required for optimum power extraction are achieved [14]—refer to Eq. (23) and Eq. (24)—then the peak-to-average power ratio can be modeled by the following expression:

$$PA_{\pm j}=1\pm\sqrt{1+\left[\frac{C_{jj}-\omega^2(M_{jj}+\mu_{jj})}{\omega\lambda_{jj}}\right]^2}=1\pm\Xi_{rj} \tag{28}$$

Equation (28) requires unconstrained motion and has been plotted in Fig. 8, but can be adapted to account for motion constraints, similar to Eq. (21). If the expression for the linear PTO-damping coefficient, when $\delta_j<1$, is inserted into Eq. (27), the following expression is obtained:

$$PA_{\pm j}=1\pm\sqrt{1+\left[\frac{C_{jj}-\omega^2(M_{jj}+\mu_{jj})}{\omega\left(\frac{A|X_j|}{\omega|\xi_j|_{\max}}-\lambda_{jj}\right)}\right]^2}$$
$$=1\pm\sqrt{1+\left[\frac{C_{jj}-\omega^2(M_{jj}+\mu_{jj})}{A\left(1-\frac{\delta_j}{2}\right)\frac{|X_j|}{|\xi_j|_{\max}}}\right]^2} \tag{29}$$

where, as the wave amplitude increases, all terms are constant except for A and δ_j. However, as A increases, δ_j decreases, which provides a nonlinear increase in the denominator under the square root. As the linear PTO-damping coefficient is increased to meet a given displacement constraint, the peak-to-average power ratio will be reduced, and the reduction is nonlinearly proportional to the increase in wave amplitude.

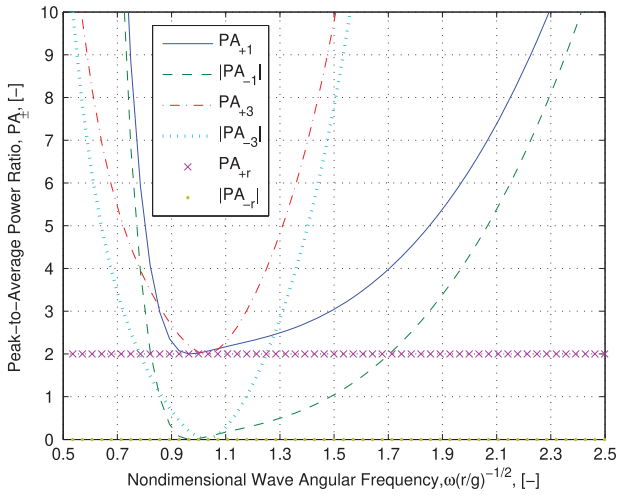

Fig. 8 The floating sphere peak-to-average power ratio for complex conjugate and resistive control

5 Power-Take-Off Force

For the WEC system to capture energy, a PTO unit must be included to provide a resistive force that acts against WEC motion. The complex PTO force amplitude, α_j, in the frequency domain can be modeled as

$$\frac{\alpha_j}{A}=\frac{[C_g+i\omega\lambda_g]X_j}{[C_{jj}+C_g-\omega^2(M_{jj}+\mu_{jj})]+i\omega[\lambda_g+\lambda_{jj}]}$$
$$=-[\lambda_g-iC_g/\omega]i\omega\xi_j=Z_{uj}i\omega\xi_j \tag{30}$$

where α_j is the complex PTO force/torque amplitude depending on the degree-of-freedom used to extract the incident wave power, and Z_{uj} is the PTO force-to-velocity transfer function. In order to estimate the magnitude of the force amplitude required by the PTO, we take the absolute value of Eq. (30) and divide it by $\omega\lambda_{jj}$:

$$\left|\frac{\alpha_j}{A}\right|=\frac{\sqrt{\left[\frac{C_g}{\omega\lambda_{jj}}\right]^2+\left[\frac{\lambda_g}{\lambda_{jj}}\right]^2}}{\sqrt{\left[\frac{C_{jj}+C_g-\omega^2(M_{jj}+\mu_{jj})}{\omega\lambda_{jj}}\right]^2+\left[\frac{\lambda_g}{\lambda_{jj}}+1\right]^2}}|X_j| \tag{31}$$

$$=\frac{\sqrt{1+\left[\frac{C_g}{\omega\lambda_g}\right]^2}}{\sqrt{1+2\left[\frac{\lambda_{jj}}{\lambda_g}\right]+\Xi^2\left[\frac{\lambda_{jj}}{\lambda_g}\right]^2}}|X_j| \tag{32}$$

If bidirectional energy flow is allowed, then the optimum phase and amplitude conditions required for maximum power extraction can be met [14], and the complex PTO force/torque amplitude can be simplified as the following expression:

$$\left|\frac{\alpha_j}{A}\right|=\frac{|X_j|}{2}\sqrt{1+\left[\frac{C_{jj}-\omega^2(M_{jj}+\mu_{jj})}{\omega\lambda_{jj}}\right]^2}=\frac{|X_j|\Xi_{rj}}{2} \tag{33}$$

The second term under the square root in Eq. (33) will always be greater than or equal to 0, resulting in the square root having a lower bound of 1 and an unconstrained upper bound. The lower bound is obtained when the wave frequency meets the floating

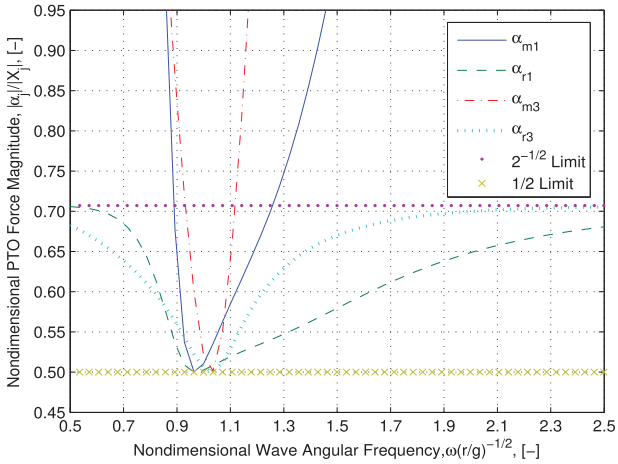

Fig. 9 The nondimensional power-take-off force amplitude for complex conjugate and resistive control of the floating sphere

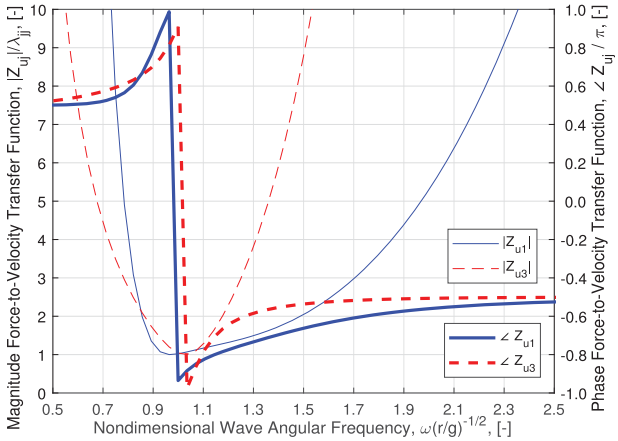

Fig. 10 The magnitude and phase of the PTO force-to-velocity transfer function for complex conjugate control

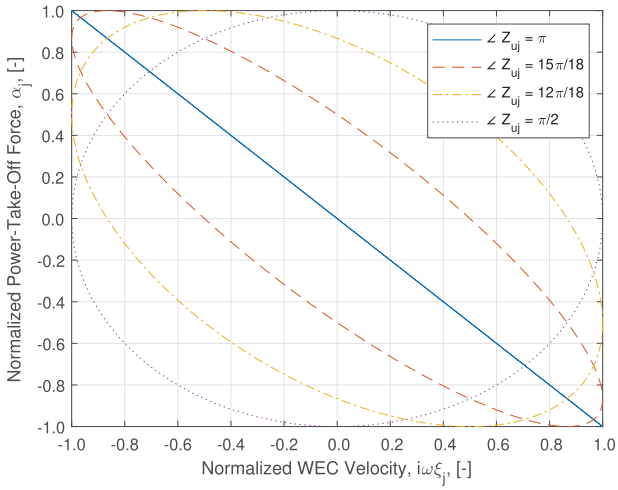

Fig. 11 Plot of the changing relationship between velocity and force with changing phase angle

body resonance frequency. Therefore, the expected PTO force under the optimum conditions for power extraction will always be greater than half of the wave-exciting force.

If bidirectional energy flow is prohibited, $C_g = 0$, and the PTO-damping coefficient is selected to optimize power absorption (refer to Eq. (8), the required PTO force will be expressed as follows:

$$\left|\frac{\alpha_j}{A}\right| = \frac{\sqrt{2}}{2}|X_j|\sqrt{\frac{\Xi_j}{1+\Xi_j}} = \begin{cases} \frac{|X_j|}{2} & \text{as } \Xi_j \to 0 \\ \frac{\sqrt{2}}{2}|X_j| & \text{as } \Xi_j \to \infty \end{cases} \tag{34}$$

For resistive control, the PTO force amplitude will vary between 1/2 and $\sqrt{2}/2$ of the wave-exciting force; see Fig. 9. Equations (33) and (34) converge to the same value when the resonant and wave frequencies match, as the conditions for optimum power extraction are met by both control schemes.

The phase and magnitude relationship of the PTO force-to-velocity transfer function can be expressed as follows:

$$\angle Z_{uj} = \arctan\left(\frac{\Im\{Z_{uj}\}}{\Re\{Z_{uj}\}}\right) = \arctan\left(-\frac{C_g}{\omega\lambda_g}\right) \tag{35}$$

whereas under complex conjugate control, the phase angle will take the following form:

$$\angle Z_{uj} = \arctan\left(-\frac{\omega[M_{jj}+\mu_{jj}] - C_{jj}/\omega}{\lambda_{jj}}\right) \tag{36}$$

The phase angle between the PTO force and WEC velocity is bounded between $\pi/2$ ($\omega \to 0$) and $3\pi/2$ ($\omega \to \infty$) and crosses π at the resonance frequency of the WEC, as shown in Fig. 10. As shown in Fig. 11, the phase angle of the optimal PTO force-to-velocity transfer function deviates from π, which corresponds to resistive control. The linear trace between the WEC velocity-to-PTO force for resistive control is no longer optimum and becomes more oblong as the ratio of the imaginary-to-real component of Z_{uj}. At the limits of $\angle Z_{uj} = \pm\pi/2$, the control command has the largest force demand when the WEC is moving at the lowest speed. Requiring high forces at low speeds can lead to issues with conversion efficiency, as the PTO systems may not be designed for optimum performance in this operating regime. Therefore, the gains over resistive control when applying complex conjugate control can be degraded with potential negative energy capture [30]. As observed in Fig. 10, at frequencies above resonance the phase angle for the heave oscillation mode decays more quickly to $3\pi/2$ than surge. Therefore, even when off resonance the surge oscillation mode requires less of a control action to tune the response of the WEC for optimum power capture, as long as the PTO is able to generate the required force.

6 Nonideal Power-Take-Off Efficiency

Complex conjugate control requires energy to flow back and forth from the oscillating body to an energy storage system, which has different losses dependent on the direction of flow of the energy flux if the PTO has a mechanical-to-electrical efficiency less than unity. If a PTO unit is selected, with a time-invariant mechanical-to-electrical efficiency defined by η_e, the resulting PTO output time-averaged power [30,31] is given by

$$P_O = \eta_e \frac{\lambda_g |i\omega\xi_j|^2}{2}[1 + e^* g^*],\ e^* = \frac{1-\eta_e^2}{\eta_e^2} \tag{37}$$

$$g^* = \frac{2G^* - \sin 2G^* - 2G\left(1-\cos^2 G^*\right)}{2\pi} \tag{38}$$

$$G = \left|\frac{C_g}{\omega\lambda_g}\right|,\quad G^* = \arctan G \tag{39}$$

where P_O is the time-averaged power, after accounting for the efficiency steps in the power conversion chain, which can be sent to the

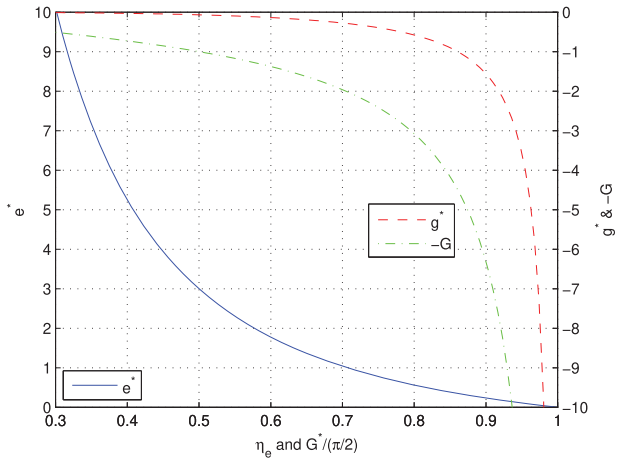

Fig. 12 The effect on e^* and g^* for a range of η_e and G values

Table 2 Limits on G as a function of η_e

η_e	e^*	$G_{e^*g^*=-1/4}$	$G_{e^*g^*=-1/2}$	$G_{e^*g^*=-1}$
0.70	1.04	1.82	2.73	4.36
0.80	0.56	2.60	4.12	7.01
0.90	0.23	4.71	8.14	14.89
0.95	0.11	8.73	16.04	30.60

grid. The peak-to-average power ratio for a nonideal PTO, $PA_{\eta_e\pm}$, can be modeled from the following equation:

$$PA_{\eta_e+} = \frac{1+\sqrt{1+G^2}}{[1+e^*g^*]}, \quad PA_{\eta_e-} = \frac{1-\sqrt{1+G^2}}{\eta_e^2[1+e^*g^*]} \tag{40}$$

The change in the e^* and g^* terms in Eq. (37), with respect to the coefficient ratio of the PTO, are shown in Fig. 12. It can be observed from Eq. (39) that the variable, G, is bounded between $[0, \infty]$ and that G^* is bounded between $[0, \pi/2]$. As observed in Fig. 12, the variable, $e^* \geq 0$, while $g^* \leq 0$, resulting in the bracketed term in Eq. (37) being bounded by $[1, -\infty]$. When the value in brackets falls below 0, there is a net flow of energy to the device rather than the grid. Inclusion of the mechanical-to-electrical efficiency can greatly reduce the time-averaged output power if care is not taken in limiting G. A new ratio of the time-averaged output power, when considering nonideal PTO efficiency between the two control strategies, can be calculated by taking the ratio of Eq. (37) when setting $\Xi_j = 1$ and with Ξ_j when $C_g = 0$, leading to the following expression:

$$\frac{P_{Omj}}{P_{Orj}} = \frac{1+\Xi_{rj}}{2}[1+e^*g^*] \tag{41}$$

As e^* and g^* are independent and can be separated in Eq. (37), it is possible to set maximum limits on G to ensure net flow of power to the grid (tabulated in Table 2). Table 2 shows that, as the PTO mechanical-to-electrical efficiency is reduced, the maximum G value for a net power output is reduced at a much greater rate. Equation (41) only requires the radiation coefficients, and the natural hydrodynamic bandwidth of the device will play a role in tempering the negative effects of PTO efficiency. Therefore, we can expect the surge oscillation mode to be less sensitive than heave when considering PTO efficiency.

7 Conclusions

This paper explores the theoretical one degree-of-freedom limits for a demonstrative floating spherical WEC. The dynamic response of the WEC considered both surge and heave modes of oscillation, as the differences in the hydrodynamic coefficients for different frequency ranges may lead to improved power capture efficiency. This follows the concept of a natural hydrodynamic bandwidth that has been shown to improve tuning of the WEC system for maximum power capture for the surge mode of motion compared to heave; however, this work does not suggest that heaving WECs are poorly designed, only that additional consideration should be taken when designing the floating body. As the work in this paper shows, the benefits of proper hydrodynamic tuning can significantly reduce the control strategy burden to maximize power capture, which can be degraded further when considering the PTO efficiency. Furthermore, to the best of our knowledge, a unique analytical expression for the PTO force amplitude was derived that provides upper and lower bounds that depend only on the wave-exciting force. Such bounds allow for rapid design iteration, as they eliminate the need to complete higher-fidelity simulations and can be calculated using frequency-domain techniques. Furthermore, analytical bounds have been placed on the ratio of the PTO spring and damping coefficients, when considering PTO efficiency, to ensure a net power output that is also strongly influenced by the natural hydrodynamic bandwidth. The final decision in selecting the WEC mode of oscillation will be completed based on the designer vision and must also consider other external factors, such as station keeping, extreme loading, power-take-off selection, and maintenance windows.

Acknowledgment

This work was authored by the National Renewable Energy Laboratory, operated by Alliance for Sustainable Energy, LLC, for the U.S. Department of Energy (DOE) under Contract No. DE-AC36-08GO28308. Funding provided by the U.S. Department of Energy Office of Energy Efficiency and Renewable Energy Water Power Technologies Office. The views expressed in the article do not necessarily represent the views of the DOE or the U.S. Government.

Conflict of Interest

There are no conflicts of interest.

Data Availability Statement

The authors attest that all data for this study are included in the paper.

References

[1] Salter, S. H., 1974, "Wave Power," Nature, **249**, pp. 720–724.
[2] Lehmann, M., Karimpour, F., Goudey, C. A., Jacobson, P. T., and Alam, M.-R., 2017, "Ocean Wave Energy in the United States: Current Status and Future Perspectives," Renewable. Sustainable. Energy. Rev., **74**, pp. 1300–1313.
[3] Drew, B., Plummer, A. R., and Sahinkaya, M. N., 2017, "A Review of Wave Energy Converter Technology," Proc. Inst. Mech. Eng., Part A: J. Power Energy, **223**(8), pp. 887–902.
[4] Weber, J., Costello, R., and Ringwood, J., 2013, "Wec Technology Performance Levels (TPLs) – Metric for Successful Development of Economic Wec Technology," Proceedings of the Tenth European Wave and Tidal Energy Conference, Aalborg, Denmark, Sept. 2–5, EWTEC.
[5] Yemm, R., Pizer, D., Retzler, C., and Henderson, R., 2012, "Pelamis: Experience From Concept to Connectiony," Philos. Trans. R. Soc. A, **370**(1959), pp. 365–380.
[6] McNatt, J. C., and Retzler, C., 2019, "The Performance of the Mocean M100 Wave Energy Converter Described Through Numerical and Physical Modelling," Proceedings of the 13th European Wave and Tidal Energy Conference. Naples, Italy, Sept. 1–6, EWTEC.
[7] Weber, J. W., Mouwen, F., Parrish, A., and Robertson, D., 2009, "Wavebob–research & Development Network and Tools in the Context of Systems Engineering," Proceedings of Eighth European Wave Tidal Energy Conference. pp. 416–420. Uppsala, Sweden. Sept. 7–10, EWTEC.
[8] Mekhiche, M., Edwards, K., and Bretl, J., 2014, "System-Level Approach to the Design, Development, Testing, and Validation of Wave Energy Converters at

Ocean Power Technologies," Proceedings of 33rd International Conference on Ocean, Offshore and Arctic Engineering, San Francisco, CA, June 8–13, American Society of Mechanical Engineers.
[9] Guerinel, M., Jansson, E., Todalshaug, J., Jesmani, M., and Guijt, K., 2017, "Modelling Alternatives for a Heaving Point Absorber With and Without Stiffness Modulation," Proceedings of twelfth European Wave Tidal Energy Conference. Cork, Ireland, Aug. 27–Sept. 1, EWTEC.
[10] Troch, P., Visch, K. D., Kofoed, J.-P., and Backer, G. D., 2010, "Application of the Time-dependent Mild-slope Equations for the Simulation of Wake Effects in the Lee of a Farm of Wave Dragon Wave Energy Converters," Renew. Energy, **35**(8), pp. 1644–1661.
[11] Whittaker, T., and Folley, M., 2012, "Nearshore Oscillating Wave Surge Converters and the Development of Oyster," Philosophical Trans. R. Soc. A, **370**(1959), pp. 345–364.
[12] Falcao, A. F. O., and Henriques, J. C. C., 2016, "Oscillating-Water-Column Wave Energy Converters and Air Turbines: A Review," Renew. Energy, **85**, pp. 1391–1424.
[13] Ringwood, J., Bacelli, G., and Fusco, F., 2014, "Energy-Maximizing Control of Wave-Energy Converters: The Development of Control System Technology to Optimize Their Operation," IEEE Control Syst. Magaz., **34**(5), pp. 30–55.
[14] Falnes, J., 2002, "Optimum Control of Oscillation of Wave-Energy Converters," Int. J. Offshore Polar Eng., **12**(2), pp. 147–154.
[15] Babarit, A., Guglielmi, M., and Clément, A. H., 2009, "Declutching Control of a Wave Energy Converter," Ocean Eng., **36**(12), pp. 1015–1024.
[16] Babarit, A., and Clément, A. H., 2006, "Optimal Latching Control of a Wave Energy Device in Regular and Irregular Waves," Appl. Ocean Res., **28**(2), pp. 77–91.
[17] Cretel, J. A. M., Lightbody, G., Thomas, G. P., and Lewis, A. W., 2011, "Maximisation of Energy Capture by a Wave-Energy Point Absorber Using Model Predictive Control," Proceedings of the Eighteenth World Congress of the International Federation of Automatic Control, Milano Italy, Aug. 28–Sept. 2, Elsevier, pp. 3714–3721.
[18] Hals, J., Falnes, J., and Moan, T., 2011, "Constrained Optimal Control of a Heaving Buoy Wave Energy Converter," ASME J. Offshore Mech. Arct. Eng., **133**(1), p. 011401.
[19] Coe, R., Bacelli, G., Wilson, D. G., Abdelkhalik, O., Korde, U. A., and Robinett, III, R. D., 2017, "A Comparison of Control Strategies for Wave Energy Converters," Int. J. Marine Energy, **20**, pp. 45–63.
[20] Sheng, W., and Lewis, A. W., 2012, "Assessment of Wave Energy Extraction From Seas: Numerical Validation," ASME J. Energy Resour. Technol., **134**(4), p. 041701.
[21] Folley, M., Henry, A., and Whittaker, T., 2015, "Contrasting the Hydrodynamics of Heaving and Surging Wave Energy Converters," Proceedings of the Eleventh European Wave and Tidal Energy Conference, Nantes, France, Sept. 6–11, EWTEC, pp. 3714–3721.
[22] Evans, D. V., 1976, "A Theory for Wave-power Absorption by Oscillating Bodies," J. Fluid. Mech., **7**(1), pp. 1–25.
[23] Wendt, F., Yu, Y.-H., Nielsen, K., Ruehl, K., Bunnik, T., Touzon, I., Nam, B.-W., Kim, J.-S., Kim, K.-H., Erik, C., Jakobsen, K., Crowley, S., Vega, L., Rajagopalan, K., Mathai, T., Greaves, D., Ransley, E., Lamont-Kane, P., Sheng, W., Costello, R., Kennedy, B., Thomas, S., Heras, P., Bingham, H., Kurniawan, A., Kramer, M. M., Ogden, D., Girardin, S., Babarit, A., Wuillaume, P., Steinke, D., Roy, A., Beatty, S., Schofield, P., Jansson, J., and Hoffman, J., 2017, "International Energy Agency Ocean Energy Systems Task 10 Wave Energy Converter Modeling Verification and Validation," Proceedings of the Twelfth European Wave and Tidal Energy Conference, Cork, Ireland, Aug. 27–Sept. 2, EWTEC.
[24] WAMIT, 2017. *WAMIT* User Manual, 7.2 ed. WAMIT, Inc., Massachusetts. See also URL http://www.wamit.com.
[25] Newman, J. N., 1962, "The Exciting Forces on Fixed Bodies in Waves," J. Res., **6**(3), pp. 10–17.
[26] Gomes, R. P. F., Lopes, M. F. P., Henriques, J. C. C., Gato, L. M., and Falcñoa, A. F. O., 2015, "The Dynamics and Power Extraction of Bottom-Hinged Plate Wave Energy Converters in Regular and Irregular Waves," Ocean Eng., **96**, pp. 86–99.
[27] Evans, D. V., 1981, "Maximum Wave-Power Absorption Under Motion Constraints," Appl. Ocean Res., **3**(4), pp. 200–203.
[28] Folley, M., Whittaker, T., and Henry, A., 2005, "The Performance of a Wave Enegy Converter in Shallow Water," Proceedings of the Sixth European Wave and Tidal Energy Conference. Glasgow, UK, Aug. 28–Sept. 2.
[29] Hals, J., Bjarte-Larsson, T., and Falnes, J., 2002, "Optimum Reactive Control and Control by Latching of a Wave-Absorbing Semisubmerged Heaving Sphere," Proceedings of the 21st International Conference on Offshore Mechanics and Arctic Engineering, Norway, Oslo, June 23–28, American Society of Mechanical Engineers, pp. 415–423.
[30] Genest, R., Félicien, B., Clément, A. H., and Babarit, A., 2014, "Effect of Non-Ideal Power Take-Off on the Energy Absorption of a Reactively Controlled One Degree of Freedom Wave Energy Converter," Appl. Ocean Res., **48**, pp. 236–243.
[31] Falcao, A. F. O., and Henriques, J. C. C., 2015, "Effect of Non-Ideal Power Take-Off Efficiency on Performance of Single- and Two-Body Reactively Controlled Wave Energy Converters," J. Ocean Eng. Marine Energy, **1**, pp. 273–286.